

Exploiting Temporal Context in High-Resolution Movement-Related EEG Classification

Jaromír DOLEŽAL, Jakub ŠTASTNÝ, Pavel SOVKA

Dept. of Circuit Theory, Czech Technical University in Prague, Technická 2, 166 27 Prague, Czech Republic

dolezja7@fel.cvut.cz, stastnj1@fel.cvut.cz, sovka@fel.cvut.cz

Abstract. *The contribution presents an application of a movement-related EEG temporal development classification which improves the classification score of voluntary movements controlled by closely localized regions of the brain. A dynamic Hidden Markov Model-based (HMM) classifier specifically designed to capture EEG temporal behavior was used. Surprisingly, HMM classifiers are rarely used for BCI design despite of their advantages. Because of this we also experimented with Learning Vector Quantization, Perceptron, and Support Vector Machine classifiers using a feature space which captures the temporal dynamics of the data. The results presented in this work show that HMM achieves the best performance due to an a priori information on physiological behavior of EEG inserted to the HMM classifier. Feature extraction process and problems with classification were analyzed as well. Classification scores of 66.7% – 94.7% were achieved in our experiments.*

Keywords

Brain-Computer Interface, EEG classification, electroencephalography, neural network applications, Hidden Markov Models.

1. Introduction

Brain-Computer Interface (BCI) is a system that bypasses traditional brain output pathways – peripheral nerves and muscles. Main target users are totally paralyzed patients which are “locked inside” without a way of communication with the rest of the world. Typical diagnose is Spiral Cord Injury (SCI) or Amyotrophic Lateral Sclerosis (ALS). In this case BCI serves as supplementation of motor functions. BCIs based on motor activity can be also used for motor recovery of partially disabled subjects, such as those after stroke [1].

A great number of BCI prototypes already exist. However, all of them suffer from too slow communication channel between a human brain and a computer working with Information Transfer Rate (ITR) lower than 100 bits per minute. If we compare this with a standard keyboard

computer interface reaching ITR of up to 1 kbit per minute we see that all these BCI devices are still not very suitable for real computer control. One possibility leading to higher ITR is the recognition of more distinct brain states – transferring more bits per state (hence high-resolution EEG recognition). However, the existing systems recognize only few very different EEG activities (left/right-hand or finger movement [2], [3], [4], [5], [6], [7], [8], mental activities [3], [9], [10], conscious EEG rhythm control [11], [12], or event-related potentials [13], [14], [15], among others).

Our research is targeted at the exploration of possibilities of the high-resolution movement recognition from an EEG signal focusing on utilization of temporal development. The aim of this paper is to investigate if voluntary movements controlled by closely localized regions of brain can be classified with a sufficient score to bring a future increase of the ITR by extending the number of classified states (movement types).

To achieve this goal we evaluate the possibility of two different movement types of the same finger (therefore high-resolution) classification at first. Movement-related EEG was selected because it is natural to control BCI with it as we commonly control our surroundings by conscious movements and because it is also possible to use it for rehabilitation [1], [16].

Further, it is known that only imagination of a movement is sufficient [17], [18] to produce the desired brain activity pattern (albeit weaker and more localized on scalp [19]) even when no feedback is present and that the brain patterns are reinforced when correct feedback is present which can further improve the performance [1]. Other advantages of the movement-related activity BCI paradigm are: the need for only a minimal initial training with a subject, a fully endogenous BCI system, and a high number of available potentially identifiable states (movement types).

Our previous work [20] showed that off-line single trial classification of extension and flexion movements of right index finger is possible using Hidden Markov Models (HMMs) classifier. The HMM classifier was specifically designed (see section 4.3) to capture movement-related EEG temporal dynamics which was not done in works [5], [6], [8].

EEG temporal dynamics is not widely used in BCI research, instead differences of signal power from different electrodes (extracted by means of appropriately defined spatial filters [21], [7]) are used by systems recognizing left and right hand movements [22], feet and tongue movements [23], or mental activities [10]. Classification of left/right-hand movements or mental activities usually addressed in BCI papers are easier tasks than classification of movements controlled by closely localized brain centers since the EEG power difference between left and right brain hemispheres can be used to obtain high classification scores. The typically used mental activities (geometric figure rotation, composition of a letter to a friend, visual counting and math problems) were specifically designed to invoke hemispheric brainwave asymmetry [10].

Experiments with movements controlled by closely localized brain centers (like finger movements) are rare – for example [24] uses imaginary closing and opening of the right hand but presents only movement detection scores. There is no other work known to us discriminating extension or flexion movements of the same finger. Classification of finger movements has been attempted so far only using invasive data acquisition methods [25]. Recent work with similar movement resolution [26] deals with extension, flexion, pronation and supination of right wrist. Interestingly, the best two-class classification score of 80% over all subjects was achieved with discrimination between extension and flexion movement. However, this work relies heavily on spatial distribution as 64 electrodes are used with Independent Component Analysis (ICA).

Further, the temporal dynamics approach enables to base the classification even on a single electrode source. Single electrode source based BCIs are usually designed for activity detection [24] rather than classification of different activities – for example work [18] uses a single source approach to detect repetitive wrist extension of right hand. Single electrode source was also used for discrimination of slow and fast extensions and rotations of right wrist work [27]. The work has shown that extension and rotation movements can be classified but provide classification score only between slow and fast movements. In addition, using EEG temporal context can also increase sensitivity to specific EEG types and facilitate extension of the system to more types of movement-related EEG in the future, therefore resulting in a high-resolution recognition.

The aim of this paper is to show that the temporal dimension alone can be used to classify closely localized movements and therefore it can improve resolution of existing movement-related BCIs when used in conjunction with the typical spatial approach as the temporal dynamics and spatial filtering are not mutually exclusive and can be combined. Our previous works presented the basic HMM architecture used to classify movements but did not show that temporal development is necessary to reach high classification score. Thus, this paper presents an exhaustive study of classification performance depending on the used classification algorithm and parameterization which is

a significant step beyond our preliminary results published in [28]. Apart from HMM, also Perceptron, Support Vector Machine (SVM), and Learning Vector Quantization (LVQ) were used as referential classification paradigms. In contrast to other studies we used all these classifiers with a feature space extended to capture temporal dynamics of movement-related EEG. We performed a detailed analysis of our results to be sure that the classification system really recognizes movement-related EEG and not e.g. EMG soaking into the used EEG.

This contribution is organized as follows: first, the properties of the used EEG database are given, and then the general properties of movement-related EEG are explained. The next section describes the methods used and classification systems architecture. The fifth section presents the achieved results and the sixth discusses problems with the classification and validity of the results. Finally, several conclusions and possible future steps are drawn.

2. Used EEG Database

The EEG database recorded in study [29] was used. Eleven subjects took part in the experiment; each of them performed brisk extension (extension followed by a return to the resting position) and flexion (flexion followed by a return to the resting position) movements of the right index finger, see Tab. 1 for total numbers of recorded epochs. Spacing between movements was 10–12 s, experimental subjects kept their eyes closed during the experiment. The EEG was recorded at a sample rate of 256 Hz by 21 AgCl electrodes placed over the left sensorimotor area with higher spatial resolution than the standard 10-10 system, see Fig. 8. All artifacts visible in the EEG signal (EOG, muscle, etc.) were localized manually and afflicted epochs were discarded. The EEG signal was filtered by a Laplacian filter with 4 neighbors mask and segmented into 10 s long epochs centered at the movement time. For more details on the experiment and EEG preprocessing see [29].

Subject n.	1	3	4	5	6	7	8	9	10	11
N. of extension	73	41	72	99	62	74	87	44	64	84
N. of flexion	81	77	38	81	66	82	63	41	74	52

Tab. 1. Total numbers of recorded epochs.

3. General Properties of the Movement-Related EEG

Volitional movements have specific responses in EEG [30]; a distinctive temporal behavior of an EEG short time spectrum can be seen, see Fig. 1:

- μ rhythm event-related desynchronization (μ ERD): the μ -rhythm is defined as an 8–12 Hz rhythm attenuated before and during the voluntary movement [30] recorded over the sensorimotor cortex. μ ERD

starts usually about 1 s prior to the movement onset [31], it is usually localized to the C3/CP3 and C4/CP4 scalp area [32] and exhibits a contralateral preponderance depending on the subject's handedness and the movement speed [32]. It is observed bilaterally. μ ERD allows differentiating not only the side of the body performing the movement, but slow and fast movements as well, and depends on the force exert by the movement [33]. The desynchronization accompanies even the mere motor imagery and is present in most normal adults' EEG [34]. Majority of papers dealing with left/right hand movement recognition utilize described preponderance of μ ERD contralateral to the performed movement.

- *β rhythm event-related synchronization (β ERS)*: central rhythms display desynchronization prior and during the movement and a rebound in the form of a phasic synchronization after the movement [17], [29]. β ERS is located about 1 s after the movement onset, see Fig. 1. ERS is larger over the contralateral hemisphere and focused slightly anterior to the focus of the largest μ ERD [29]. Both μ and central β rhythms are products of the idling sensorimotor cortex, μ rhythm is generated in the somatosensory area, β rhythm in the motor area [35]. The amplitude and focus of the β ERS also allows distinguishing between types of movements [29], the amplitude is greater and focus larger in finger extension-flexion compared to flexion-extension movement.
- *μ rhythm event-related synchronization and β rhythm event-related desynchronization* can be also observed in Fig. 1. but their contribution to the movement classification is not significant in this case.

The described behavior of movement-related EEG is further utilized by our HMM-based classification system, see Fig. 1 and description of the classifier below.

4. Methods

4.1 EEG Modeling

The used EEG database was originally recorded for a physiological research. From our point of view it has one significant drawback: there is no continuous non-movement-related (resting) EEG recording of sufficient length in the database, and thus we were unable to evaluate false movement detection ratio. We decided to generate an artificial resting EEG signal by AR modeling [36], [37] to at least partially overcome this limitation. The 8th order AR model parameters were estimated from short segments (3 s located -4.5 to -1.5 s prior to the movement onset) of the resting EEG preceding each movement present in the database. Since our interest was to model a typical resting EEG signal for a given subject and electrode we computed one model for each subject and each electrode. The model coefficients were obtained from autocorrelation function

averaged across all the appropriate realizations of EEG. The modeled signal was obtained by filtering white noise with the modeling filter and scaling to the average power of the training data. For each subject, the numbers of extension and flexion realizations were averaged and the same numbers of 10 second long resting EEG realizations were generated [37] and imported into the database. We used the classification score time courses (see section 5.2) to show that the resting EEG was generated correctly with respect to the used feature extraction methods. If there were any undesired differences between the modeled and real EEG they would be visible in Figs. 3b, 4b, or 5b, as flat classification time course, see section 6.1. Currently, we have been recording a new EEG database under less controlled conditions including also resting EEG and the first classification experiments gave results very similar to the ones presented below justifying the correctness of the used modeling approach [38].

4.2 Feature Extraction

The feature vectors for classification were computed from 1 s long rectangular window sliding with a step of 183 ms. The following features were tested:

- *Discrete Time Fourier Transform (DTFT)*: frequency band 6 – 40 Hz was used for classification since the movement-related changes in EEG can be found in this band. The frequency resolution of FFT was of 1 Hz and the dimension of the feature vector was thus 35. FFT algorithm was used.
- *Autoregressive Model (AR) coefficients*: AR model of the 8th order [37] was used to capture the 1 – 43 Hz band. This was achieved by decimating the signal three times prior to the modeling to cover only the frequency band where the EEG changes accompanying movement can be found. Autocorrelation method was used for extracting the AR features.
- *Cepstrum*: 8 coefficients of real cepstrum were computed from the AR model coefficients (LPC cepstrum). This method was selected as it is less sensitive to noise than DFT cepstrum and coefficients are less mutually correlated [39]. It is possible to separate periodic and non-periodic components of the original signal using cepstral coefficients. This can be of use with EEG processing as movement-related EEG can be viewed as rhythmic μ -rhythm passing through additional attenuating or amplifying filtering to get the ERD/ERS described above.
- *Reflection coefficients*: 8 reflection coefficients were derived from the AR models using Levinson-Durbin recursion [40]. Reflection coefficients have physical interpretation as intensities of reflected waves' propagation through medium. The same reasoning as for cepstral coefficients can be also applied here.

The similarity of a signal power spectrum and the Euclidean distance in the feature space is less correlated

with the AR coefficients. Therefore we say that the AR coefficients do not constitute Euclidean Distance Feature Space (EDFS) as the remaining features. Due to this, the relation between AR coefficients and the signal power spectra is nonlinear; this can result in lower performance when a classifier utilizing the Euclidean distance function is used. Since our classifier relies on the temporal development of the EEG signal described above we also experimented with features extended with the approximation of their first derivative (Δ) parameters. The derivative was computed from several time frames by polynomial approximation used in speech processing [41] to reduce its sensitivity to noise.

4.3 Classifiers Used

Our previous very preliminary results [28] showed that HMMs are able to utilize the underlying temporal development in the movement-related EEG signals to classify movements controlled by closely localized brain centers. Classification system based on HMM [42] was reused from our previous work [20]. Hidden Markov Models are dynamic and generative classifiers widely used in speech recognition. HMMs are designed for classifying time series [42] and capable of modeling sudden changes in the dynamics of the data which is frequently observed in physiological data. Despite of this, HMMs are rarely used with biomedical data such as ECG, respiration rate, and EEG [43].

The architecture of the used HMMs is designed to capture the temporal development of movement-related EEG. The used models have the left-to-right, no skips architecture with four emitting states modeling the four significant phases of movement-related EEG, see Fig. 1 and the description of the EEG properties above. The second emitting state of the model is usually trained to the movement-related μ ERD, and the third emitting state to μ ERS or β ERS depending on the individual response of a given experimental subject, see Fig. 1. The first and last emitting state model the resting states before and after the movement (called “silence” in Fig. 1 to avoid confusion with the real resting type of EEG). No skips are introduced into the model structure as we do not expect that any of the movement-related phases can be omitted (based on results presented in [29], [31] and other works); simple left-to-right architecture is used as phases follow each other in the described sequence. The emitting states emit a vector of the same dimensionality as the input feature vector, single Gaussian mixture models with diagonal covariance matrix are used for definition of the output probability distribution function. Hidden Markov Toolkit [41] was used to implement the HMM classifier.

The described approach has several advantages [44]: *utilization of the context information*: the system uses the temporary context of the EEG to improve the classification score; *physiological compatibility*: the selected model ar

chitecture matches the underlying physiological process and it is even possible to segment the EEG with the help of the HMM classifier (on the base of the trained transition matrices) [45], [46]; *ease of the interpretation*: it is quite simple to interpret the contents of the trained model. This is a great advantage compared to e.g. some kinds of neural networks where the implementation of the trained system is not so straightforward; and, finally, *ability to model the EEG*: we are able to generate synthetic realizations of the EEG for tests of various algorithms. None of these advantages can be reached with neural network-based classifiers.

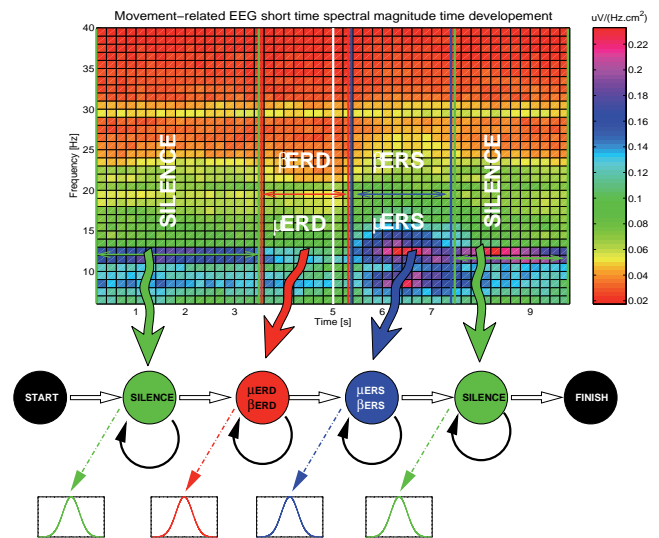


Fig. 1. Model architecture along with the EEG short time spectrum temporal development; subject 4, right index finger extension, electrode 6.

Compared to other works using HMM for EEG classification ([5], [6], [47] among others) we designed the HMM architecture with respect to the temporal development of movement-related EEG. The movement-related EEG signal is thus not recognized based on μ ERD spatial scalp distribution but on its temporal context using only one signal source – based on differences between μ ERD and β ERS parameters between both types of movements. Model architecture designed according to EEG behavior is actually an insertion of a priori information on the EEG behavior to the classification system. Further, always only one signal source – electrode – is used to classify the type of movement. However, neural network-based classifiers are very frequently used by BCI systems [48]. To see whether the whole HMM framework brings an advantage we also dealt with LVQ, Support Vector Machine (SVM), and Perceptron extended to capture the temporal dynamic of the EEG signal by feature vector concatenation (similar to the Time Delayed Neural Network (TDNN) approach). Signal features from 1, 3, and 5 segments were concatenated together with segment step of 366 ms (i.e. each second segment was skipped) giving sequences of features covering 1, 1.74, and 2.47 seconds, see Fig. 2 for an example.

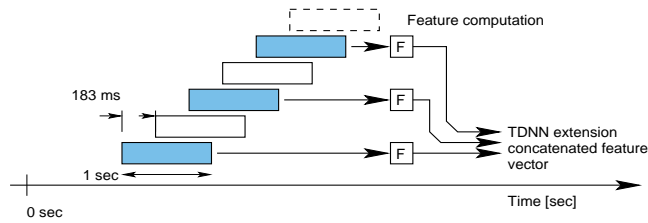


Fig. 2. TDNN-like segmentation and feature extraction process.

No concatenation of features was needed to be performed with the HMM classifier, as it supports classification of time series natively. The Perceptron, SVM, and LVQ classifiers were trained at the time intervals $<+0.14\text{ s}; +1.14\text{ s}>$, $<-0.22\text{ s}; +1.51\text{ s}>$, and $<-0.59\text{ s}; +1.87\text{ s}>$ relative to the movement offset for sequence lengths of feature vector 1, 3, and 5 segments respectively. The chosen training time intervals contain both ERD and ERS, since the maximum ERD power decrease is usually from 0 to 0.1 s after the movement time [31], and the maximum of ERS power increase is usually from 1 to 1.5 s after the movement time (hence 1, 3, and 5 frames for TDNN-like extension), see Fig. 2. The detailed descriptions of application of the chosen neural networks classifiers follow:

- *Perceptron* – as the simplest available classifier – was intentionally used to see if it could be used for fast and reliable *movement detection* (movement-resting two-class classification).
- *SVM* is considered to be the most suitable classifier [48] in the field of BCI. SVM has good generalization properties and low sensitivity to overtraining for features with high dimensionality [49]. SVM is also partially resistive to the *curse of dimensionality* and is a stable classifier. Radial Basis kernel Function (RBF SVM) was used in our study as this kernel is generally used in BCI research with good results [48], [50]. Sequential Minimal Optimizer (SMO) learning algorithm was applied because it is conceptually simple, generally faster, and has better scaling properties for difficult SVM problems than the standard SVM training algorithm [51].
- *LVQ* network is commonly used for classification of movements on the opposite side of the body [52] or their detection [53]. LVQ network defines the boundaries between classes based on prototypes representing output classes, the nearest neighbor paradigm and winner takes all strategy [54]. LVQ is also partially resistive to the curse of dimensionality. The amounts of data per classes were balanced in order to obtain unbiased results.

As Perceptron does not natively support three-class classification (flexion, extension, and resting) and both SVM and LVQ did not give sufficiently good and valid classification results with three classes we present detailed results of three-class classification only for HMMs and only two-class classification results (extension/flexion –

movement classification and extension/resting – *movement detection*) for the remaining classifiers. *Movement classification* and *movement detection* results are also present with HMM to have referential results. A complete framework for EEG processing implemented in Matlab, C++, and Linux command line shell was built. The following parts make up the core of the system:

1. *Feature extraction* was written in Matlab; for EEG raw format reading we used function *dread* from toolbox [55]. The input to this block is the raw EEG. The output is parameterized feature vector.
2. *Randomization procedure* is responsible for the mitigation of the effect of the small training and testing set – to combat the *curse of dimensionality*. The amount of data needed to describe the class increases exponentially with the dimensionality of the feature vectors [56]. However, the training set is usually very small because of demanding and time consuming EEG recording. Holdout with stratification [57] was used to get reliable results independent on the training and testing EEG realizations [45], [20]. Each classification was run 16 times with different (and random) division of EEG realizations between the disjunctive training (50% of realizations) and testing (50% of realizations) sets.
3. *Classification module* using the HMM, SVM, LVQ, and Perceptron.
4. *Evaluation module* collected the 16 results of independent runs and computed averages and standard deviations of the classification scores. Only those aggregated numbers were used for the comparison.

Testing of the classification performance was performed using the moving segment method to detect possible false positive classification results (see section 6.1) because a reliable classifier must reach the best classification score using the EEG segments close to the time of the real movement.

5. Results

5.1 Hidden Markov Models

HMMs successfully classify movement types and also give the best results for movement detection. Results of the three-class classification are shown in Tab. 2. The left half of the table contains the classification scores computed as an average from extension, flexion, and resting classification for the given subject and parameterization. The best score is in boldface; the right half of the table contains detailed scores for extension, flexion, and resting type of movement for the best result along with the best electrode. The classification with reflection coefficients gave the same results as the classification with cepstral coefficients; thus the appropriate column was removed from the table

for the sake of space. Results reached with AR+Δ, CEP+Δ, K, and K+Δ parameters are also not presented as using these features did not improve classification score at all.

S.	FFT	F+Δ	AR	CEP	Extension	Flexion	Resting	E.
1	78.6	77.6	61.2	70.0	66.5±14.5	69.1±16.2	100.0±00.0	10
3	85.5	86.2	65.3	80.4	82.0±07.4	77.5±05.3	99.0±02.5	6
4	96.6	95.6	84.7	90.4	92.5±06.0	97.2±02.3	100.0±00.0	10
5	86.1	85.1	79.8	89.6	81.2±15.3	77.1±08.7	100.0±00.0	10
6	87.6	87.5	74.1	80.7	74.9±09.2	88.0±08.3	100.0±00.0	17
7	84.6	85.2	65.3	79.8	67.6±03.4	88.0±04.9	100.0±00.0	17
8	97.2	97.4	58.7	84.0	93.7±03.6	100.0±00.0	98.5±03.0	12
9	85.6	85.8	63.4	76.4	77.5±13.9	79.9±07.8	100.0±00.0	15
10	89.1	87.2	66.3	77.0	94.2±05.7	77.2±12.5	95.9±02.8	5
11	94.4	92.2	64.6	92.4	90.7±10.6	97.3±02.5	95.4±03.7	5

Tab. 2. Three-class classification results, HMM classifier with all the parameterizations.

S.	FFT	FFT+Δ	AR	CEP	Extension	Flexion	E.
1	62.8	62.5	52.6	55.7	69.2±13.6	56.4±15.7	12
3	74.7	75.0	79.7	85.7	84.4±06.4	87.0±05.2	16
4	92.6	92.4	87.0	92.0	94.3±05.2	90.9±06.1	17
5	81.2	81.7	80.8	84.7	78.9±08.7	90.4±08.6	10
6	81.7	81.2	63.4	70.5	86.0±08.8	77.4±09.2	17
7	77.4	77.6	69.1	79.2	92.3±04.3	62.9±08.4	6
8	98.5	97.4	76.9	87.3	100.0±00.0	97.1±02.5	10
9	71.1	71.2	71.4	71.3	72.4±11.2	70.5±10.7	6
10	81.3	80.0	71.0	74.8	81.5±14.3	81.1±18.4	11
11	93.6	92.7	77.4	93.1	97.5±03.2	89.7±08.6	6

Tab. 3. Movement classification results, HMM Classifier with all the parameterizations.

Results of the two-class classification experiments: movement classification and movement detection are shown in Tabs. 3 and 4. The features giving the best classification results with HMM classifier are mostly FFT or FFT+Δ; the worst results were achieved with AR coefficients.

S.	FFT	FFT+Δ	AR	CEP	Extension	Resting	E.
1	99.8	99.8	95.1	99.5	99.6±01.0	100.0±0.00	10
3	100.0	100.0	89.2	97.1	100.0±0.00	100.0±0.00	6
4	100.0	100.0	98.9	100.0	100.0±0.00	100.0±0.00	5
5	100.0	100.0	88.6	97.7	100.0±0.00	100.0±0.00	10
6	100.0	100.0	99.4	95.3	100.0±0.00	100.0±0.00	5
7	100.0	100.0	87.6	96.7	100.0±0.00	100.0±0.00	5
8	100.0	100.0	86.8	99.0	100.0±0.00	100.0±0.00	10
9	100.0	100.0	82.4	90.8	100.0±0.00	100.0±0.00	7
10	99.3	99.1	80.6	92.5	99.0±01.9	99.6±01.0	17
11	99.8	99.8	82.7	97.1	100.0±00.0	99.6±01.0	6

Tab. 4. Movement detection results, HMM classifier with all the parameterizations.

5.2 Perceptron, Support Vector Machine, and Learning Vector Quantization

The results achieved by the Perceptron, SVM, and LVQ classifiers are presented in Tabs. 5 and 6. The left half of Tab. 5 contains the classification scores computed as an average from extension and flexion classification for the given subject and classification system. The best score is in boldface; the right part of the table contains the best scores with confidence intervals, parameterization, number

of concatenated feature vectors, movement time offset interval, and electrode at which the best score was reached. Only the results for the number of concatenated feature vectors and parameterization resulting in the highest classification score are shown for the sake of space. C is the number of concatenated feature vectors, PAR is the parameterization. As we classified data obtained from a sliding window, we added the time interval in which the best classification score was reached.

S.	PCT	SVM	LVQ	PAR	C	Extension/Flexion	Time offset	E.
1	72.8	63.4	62.0	FFT+Δ	3	71.3±10.4/74.1±07.2	-0.41-+1.33	11
3	68.3	71.8	74.1	CEP/K	3	69.8±08.8/78.5±05.1	-0.78-+0.95	16
4	82.7	88.9	77.6	FFT+Δ	5	96.3±04.9/81.3±07.9	-0.22-+2.25	12
5	69.7	77.2	73.4	FFT+Δ	5	70.3±04.5/84.1±04.0	-0.41-+2.06	11
6	63.2	66.3	59.0	CEP	1	63.9±11.7/68.5±10.3	0.14-+1.14	11
7	72.3	75.8	74.2	FFT	5	80.0±10.5/72.0±12.1	1.06-+3.53	6
8	68.3	72.9	83.9	FFT	5	87.7±06.1/80.1±04.8	-1.33-+1.14	6
9	64.2	69.7	61.4	K	5	73.8±10.0/65.2±13.0	-1.33-+1.14	6
10	74.5	77.8	71.2	FFT	5	78.4±10.2/77.4±07.4	-0.59-+1.88	11
11	76.5	78.8	76.9	K	5	82.6±05.2/70.8±09.8	-0.59-+1.88	6

Tab. 5. SVM, PCT and LVQ movement classification results.

The fact that it contains the time of the movement in 8 of 10 subjects and near post-movement interval indicates that the classification is based on movement-related EEG and not on any other unwanted artifactual features. Finally, in all but only three cases, using five frames for classification gave the best results showing the need for the temporal dynamics of the movement-related EEG signal to get better classification results. The features giving the best classification results are again the FFT or FFT+Δ (11 out of 20 experiments). AR and AR+Δ never achieved the best results, which underlines the importance of the existing EDFs for the classification.

S.	PCT	SVM	LVQ	PAR	C	Extension/Resting	Time offset	E.
1	84.2	85.4	80.2	CEP	5	82.0±06.4/88.6±05.8	-0.59-+1.88	7
3	96.1	96.0	89.5	CEP	5	95.4±05.9/96.6±03.7	-0.59-+1.88	16
4	95.2	96.8	89.8	FFT+Δ	5	95.0±05.4/99.1±01.7	-0.41-+2.06	16
5	97.3	97.4	96.2	CEP	5	95.8±02.6/99.0±01.6	-0.41-+2.06	11
6	94.2	95.7	88.5	FFT	5	94.3±05.0/96.6±03.5	-0.41-+2.06	6
7	95.8	97.3	88.7	FFT+Δ	5	95.5±02.8/99.0±01.6	-0.59-+1.88	10
8	99.0	100.0	98.7	CEP	5	100.0±0.00/100±0.00	-0.59-+1.88	10
9	84.4	93.4	83.3	FFT+Δ	5	94.3±05.0/92.5±09.8	-0.78-+1.69	6
10	95.7	96.1	95.2	FFT+Δ	5	95.8±03.2/96.5±02.7	-0.78-+1.69	10
11	94.3	95.2	88.1	CEP	5	97.4±02.5/92.6±04.3	-0.59-+1.88	6

Tab. 6. SVM, PCT and LVQ movement detection results.

The time developments of the best score achieved by Perceptron are shown in Fig. 3. We can see a rise of the classification score at/after the time of the movement (marked by a black vertical line). The classification score reached by the SVM is higher compared to the results obtained by the Perceptron classifier thanks to more complex SVM architecture, see Tabs. 5 and 6.

Examples of the classification score time development of the SVM are shown in Fig. 4. Note that the partial classification between extension and flexion movement can be seen, although the achieved score is lower and less stable than with movement detection.

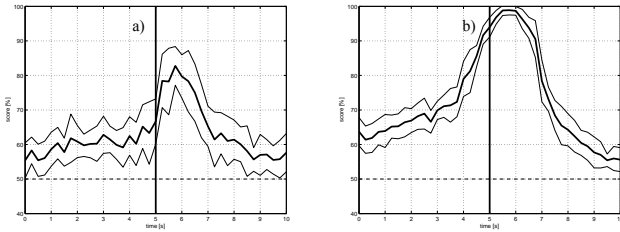


Fig. 3. Perceptron classification score with 95% confidence intervals a) movement classification, subject 4, electrode 12, FFT features; b) movement detection, subject 8, electrode 15, cepstral features.

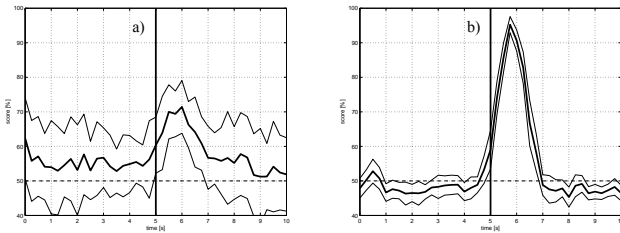


Fig. 4. SVM classification score with 95% confidence intervals a) movement classification, subject 10, electrode 10, FFT+ Δ features; b) movement detection, subject 11, electrode 6, cepstral features.

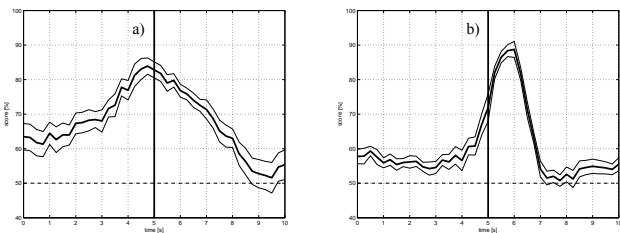


Fig. 5. LVQ classification score with 95% confidence intervals a) movement classification, subject 8, electrode 6, FFT features; b) movement detection, subject 7, electrode 11, cepstral features.

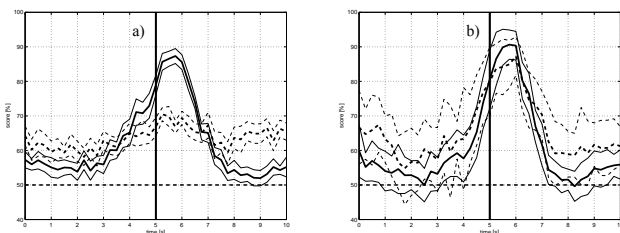


Fig. 6. Movement detection classification score with 95% confidence intervals. Comparison of cepstral (solid line) and AR (dashed line) features; subject 6, electrode 6, a) LVQ classifier b) Perceptron classifier.

Examples of the classification score time development for the LVQ network are shown in Fig. 5. Note that the LVQ movement classification gives more stable results than the Perceptron and SVM classifiers.

The EDFS is crucial for LVQ – the classification based on AR coefficient gives worse results than with the Perceptron and SVM classifiers because the AR coefficients does not constitute an EDFS. Perceptron and SVM are less afflicted, compare Figs. 6a and 6b.

6. Validation of Results

Validation of results is mandatory when we work with noisy and non-stationary biomedical signals. We analyzed placement of the electrodes achieving the best score and we did visual inspection of the classification scores and short-time spectra temporal developments.

6.1 Problems with Classification

We encountered few cases of false positive classification results when the classifier gave correct classification results due to systematical artifactual differences (SAD) in the recorded data. SADs likely came from the block recording – all the extension movements were recorded in one block and flexion movements in another block, see [31].

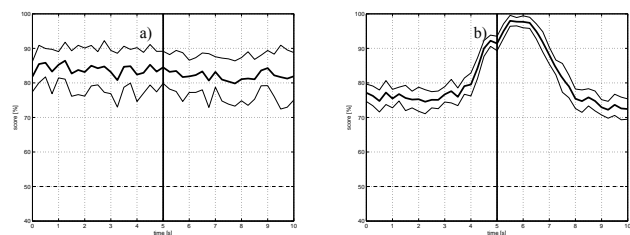


Fig. 7. SVM, FFT features a) false positive - movement classification, subject 9, electrode 5, removed from experiments, b) positive movement detection classification, subject 5, electrode 11.

This complicated interpretation of the results. First, it was necessary to make sure that the feature extraction had been set up properly to capture only the movement-related EEG and not any undesired differences (e.g. technical artifacts). Second, we had to carefully examine all our results and related EEG for the presence of classification artifacts. Based on our findings, we completely removed subject 2 (we detected an artificial 30 Hz rhythm in all the extension movement epochs independent on the movement) and electrodes 5 and 10 of subject 9 from our analysis, see Fig. 7a.

However, a small portion of the false positive classification results from the block recording remained as can be seen in Figs. 3a, 4a, and 5a. These were assessed by the *score gain* – the difference of the maximal classification score reached close to the time of the movement and the classification score in the resting period 5–4 s before the movement onset which clearly indicates whether the classifier reacts to the movement. All the temporal developments of classification scores were manually inspected and only the true positive results (showing the significant classification *score gain*) were taken into account. We shall emphasize here that these SADs were of static character and do not have any impact on results presented in [31]. On the contrary, the classification results of the artificial non-movement data were frequently seemingly false positive as the resting class can be classified successfully, regardless of the movement offset (it is stationary in the whole 10 s

period), e.g. giving working classification (100% score) for the resting class and random classification (50% score) for the movement class anywhere in the time period of 5 – 4 seconds before the movement onset. Since the classification score is computed as weighted average of the scores for the two classes, in case of movement detection the classification score baseline can be of up to 75%, see Fig. 7b for an example of positive movement detection classification result. The movement is detected as we can see the score gain around the movement time.

6.2 Localization of the Electrodes

Based on the electrode locations, we can deduce which EEG movement-related phenomenon was used for the classification. As both movements are controlled primarily by the contralateral sensorimotor cortex, the most suitable electrodes should be those overlying the contralateral sensorimotor hand area (electrode C3 and its surroundings) [29]. The ERD shows significant differences between the two types of the movements in both pre-movement and post-movement periods [31] at electrodes 10 (C3) and 11 where also maximum of μ ERD is located. According to work [29] the maximum of ERS is located at electrodes 5 and 6. Indeed, electrode 6 was the most frequently used and electrode 10 was the second most frequently used over all experiments. See Fig. 8 for electrode placement used in our experiments.

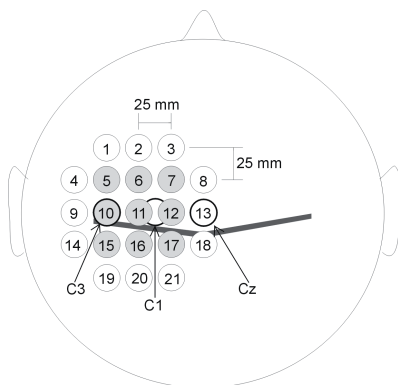


Fig. 8. Electrode placement on scalp. Gray circles indicate the 9 source derivations analyzed in our study. Approximate position of the central sulcus separating the primary motor cortex from the primary somatosensory cortex is marked by a gray line.

The locations of the electrode giving the best classification score for three-class classification as well as *movement classification* (electrode 10 – C3 – for 5 experiments) shows that the HMM classification system mostly utilizes μ ERD to distinguish between both types of movements and resting EEG, see Tabs. 2 and 3. Furthermore, the electrodes giving the best classification scores for *movement classification* with referential classifiers are the electrode 11 (4 times out of 20 experiments) where ERD is most likely found [31] and electrode 6 (4 times where ERS is most likely found [29]).

However, the results are slightly different when we perform *movement detection*, see Tabs. 4 and 6. The locations of the best electrodes are more evenly spread across all the nine locations used for classification. This can be explained by the bigger differences between resting and movement-related EEG compared to two movement-related EEG classes. The classification results varied across the electrodes used for classification and experimental subjects. Manifestation of movement-related activity is highly individual so the electrode giving the best classification has to be individually found. For example, with subject 11 where the movement-related activity is very localized the best score was always reached around electrode 6 where ERS is located, see Fig. 9.

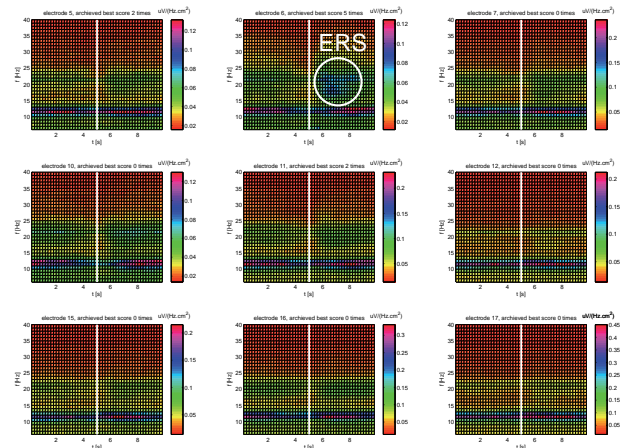


Fig. 9. Extension movement-related activity for all the electrodes of subject 11. All the classifiers utilized ERS localized around electrode 6.

The centroid of the electrodes giving the best classification scores over all experiments is located 5.35 cm left of Cz and 0.5 cm frontally of the Cz electrode. The positions of the electrodes achieving the best classification scores as well as the localization of time windows with TDNN-extended neural networks are in correspondence with the results published in physiological studies summarized in section 3. This proves that the classifiers use movement-related EEG for classification and not e.g. EMG soaking into recorded EEG signal.

7. Comparison of Results

The HMM achieved the best results, see Tab. 7.

Classifier	Ext/Flex/Rest	Ext/Flex	Ext/Rest
HMM	88.7 ± 5.84	83.0 ± 10.7	99.9 ± 00.2
Perceptron	Not applicable	71.2 ± 11.6	93.6 ± 05.3
SVM	51.7 ± 14.2	74.3 ± 08.9	95.4 ± 03.4
LVQ	61.4 ± 11.6	71.3 ± 08.8	90.3 ± 03.7

Tab. 7. Grand averages of the best classification scores in percents reached by our experiments.

We surmise this is due to the usage of longer epochs and even more dynamic approach than our TDNN-like

extension – consider 2 classes with same mean duration but different standard deviations: HMMs include this deviation into the likelihood of the class. On the other hand, discriminative classifiers do not take this directly into account [48]. The results reached by static classifiers are comparable, Perceptron achieved the least stable results.

As the best signal features for the next experiments with HMM, the FFT (22 times out of 30 experiments) and FFT+ Δ (5 times) were chosen (see Tabs. 2, 3 and 4). The FFT and FFT+ Δ features were also the best features with TDNN-extended static classifiers and *movement classification* task; they have achieved the best score with 6 out of 10 experimental subjects (see Tab. 5). For *movement detection* task, (see Tab. 6) the cepstral coefficients performed the best (5 times) followed by FFT+ Δ (4 times) and FFT (1 times). In this case the superiority of cepstral coefficients can be attributed to the separation of periodical and aperiodical signal components. The AR coefficients were not proven useful; clearly the features constituting the EDFs are better for classification. This is crucial for the LVQ classifier; Perceptron and SVM were less afflicted by missing EDFs (see Fig. 6).

The TDNN-like extension capturing temporal dynamics helped to reach higher classification score. The best score was achieved only 1 time without the extension (see Col. 5 in Tab. 5) and 2 times with classification extended to 3 time frames with *movement classification* task for all the experimental subjects (see Col. 1 and 2 in Tab. 5). Using 5 frames gave the best results in all remaining cases and also with *movement detection* task. Three-class classification was not applicable for the Perceptron classifier and the classification with SVM achieved unsatisfactory results as SVM is not inherently designed for three-class problems. Results achieved with the LVQ classifier were also unsatisfactory: while the resting EEG was classified correctly, the movement-related EEG was frequently classified as resting.

8. Conclusions and Next Steps

The work compares various approaches to movement-related EEG classification of closely localized movements.

Classification system based on HMM achieves the highest classification score. The a priori information inserted into the HMM architecture helps to increase recognition score compared to the standard neural network classifiers even with TDNN-like extension.

Static classifiers using a feature space which captures the temporal dynamics of the data were found suitable for *movement detection* but classification scores reached with *movement classification* were too low for practical application. However, they can be used to parameterize an EEG signal to get an additional feature space dimension for the HMMs indicating ongoing movement (like voice activity detector for the speech processing).

Classification scores achieved in our experiment are comparable with discriminating extension and flexion of right wrist [26], unfortunately, works [27] and [24] did not provide classification scores between the different movement types. Our overall results are proven as credible by the detailed analysis of the database and classification results.

We showed that classification of closely localized movement of the same limb is possible, which is important for utilization in rehabilitation [16]. The proposed classification system is also expected to be able to work with imagined movements as demonstrated in [18]. Finally, since it uses the temporal developments of EEG signals, it also should be easily extendable to classify different types of movements allowing a high-resolution EEG-based movement classification.

The classification works using only one signal source, which is also an improvement comparing to a need for all the scalp potentials used in traditional common spatial filter-based approach.

We have shown that classification of closely localized movements is possible solely on the base of their temporal development. We expect that using the additional temporal dimension will improve resolution of existing BCI systems mostly utilizing the spatial approach as dynamic classification can be also applied to reconstructed movement-related EEG by PCA or ICA, or directly to the movement-related components.

Currently, we have been recording a new EEG database without drawbacks present in the EEG database used in this paper. The new database is recorded under less controlled conditions in order to make the procedure closer to the real BCI use and contains movement-related EEG of flexion and extension movements of index fingers of both hands to further increase the number of recorded EEG states. Our first results with HMM and FFT features are in compliance with the results presented in this paper. Although the achieved classification scores with the new database are lower than those presented in this paper yet, finger extension and flexion movements are distinguishable. We will incorporate the ICA in our future experiments in order to assess the performance of both temporal and spatial approach.

Acknowledgements

This work has been partially supported by the research program Transdisciplinary Research in Biomedical Engineering II No. MSM 684 0770012 of the Czech Technical University in Prague, and the Grant GACR 102/08/H008: Biological and Speech Signal Modelling. Our gratitude belongs to Prof. Andrej Stančák (The 3rd Medical Faculty of the Charles University in Prague) who provided us with the EEG database.

References

- [1] NEUPER, C. Feedback-regulated mental imagery in BCI applications: Using non-invasive EEG and NIRS signals. In *BCI Workshop 2009 – Advances in Neurotechnologies*. Berlin (Germany), 2009.
- [2] BLANKERTZ, B., DORNHEGE, G., KRAULEDAT, M., MULLER, K. R., KUNZMANN, V., LOSCH, F., CURIU, G. The Berlin brain-computer interface: EEG-based communication without subject training. *IEEE Transactions on Neural Systems and Rehabilitation Engineering*, 2006, vol. 14, no. 2, p. 147-152.
- [3] PENNY, W. D., ROBERTS, S. J., STOKES, M. J. EEG-based communication: a pattern recognition approach. *IEEE Transactions on Rehabilitation Engineering*, 2000, vol. 8, no. 2, p. 214-215.
- [4] SCHLOGL, A., LUGGER, K., PFURTSCHELLER, G. Using adaptive autoregressive parameters for a brain-computer interface experiment. In *IEEE 19th Annual International Conference on Engineering in Medicine and Biology Society*. 1997, vol. 4, p. 1533-1535.
- [5] CINCOTTI, F., SCIPIONE, A., TINIPERI, A., MATTIA, D., MARCIANI, M. G., MILLAN, R., SALINARI, S., BIANCHI, L., BABILONI, F. Comparison of different feature classifiers for brain computer interfaces. In *Proceedings of the 1st International IEEE EMBS Conference on Neural Engineering*. 2003, p. 645-647.
- [6] HE SHENG, L., XIAORONG, G., FUSHENG, Y., SHANGKAI, G. Imagined hand movement identification based on spatio-temporal pattern recognition of EEG. In *International IEEE EMBS Conference on Neural Engineering*. 2003, p. 599-602.
- [7] MCCORMICK, M. S., MA, R., COLEMAN, T. P. An analytic spatial filter and Hidden Markov Model for enhanced information transfer rate in EEG-based brain computer interfaces. In *IEEE International Conference on Acoustics, Speech, and Signal Processing (ICASSP)*. Dallas (TX, USA), 2010.
- [8] OBERMEIER, B., GUGER, C., NEUPER, C., PFURTSCHELLER, G. Hidden Markov Models for online classification of single trial EEG data. *Pattern Recognition Letters*, 2001, no. 22, p. 1200-1309.
- [9] ANDERSON, C. W., STOLZ, E. A., SHASUNDER, S. Discriminating mental tasks using EEG represented by AR model. In *IEEE 17th Annual Conference on Engineering in Medicine and Biology Society*, 1995, vol. 2, p. 875-876.
- [10] ANDERSON, C. W., SIJERČIĆ, Z. Classification of EEG signals from four subjects during five mental tasks. In *Proceedings of the Conference on Engineering Applications in Neural Networks (EANN '96)*, 1996, p. 407-414.
- [11] WOLPAW, J. R., BIRBAUMER, N., MCFARLAND, D. J., PFURTSCHELLER, G., VAUGHAN, T. M. Brain-computer interfaces for communication and control. *Clinical Neurophysiology*, 2002, vol. 113, no. 6, p. 767-791.
- [12] WOLPAW, J. R., MCFARLAND, D. J., VAUGHAN, T. M. Brain-computer interface research at the Wadsworth center. *IEEE Transactions on Rehabilitation Engineering*, 2000, vol. 8, no. 2, p. 222-225.
- [13] BAYLLIS, J. D., BALLARD, D. H. Recognizing evoked potentials in a virtual environment. *Advances in Neural Information Processing Systems*, 2000, vol. 12, p. 3-9.
- [14] SCHALK, G., WOLPAW, J. R., MCFARLAND, D. J., PFURTSCHELLER, G. EEG-based communication: presence of an error potential. *Clinical Neurophysiology*, 2000, vol. 111, no. 12, p. 2138-2144.
- [15] HOFFMAN, U., VESIN, J. M., DESERENS, K., EBRAHIMI, T. An efficient P300-based brain computer interface for disabled subjects. *Journal of Neuroscience Methods*, 2008, vol. 167, p. 115-125.
- [16] VUCKOVIC, A. Non-invasive BCI: How far can we get with motor imagination? *Clinical Neurophysiology*, 2009, vol. 120, no. 8, p. 1422-1423.
- [17] MCFARLAND, D. J., MINER, L. A., VAUGHAN, T. M., WOLPAW, J. R. μ and β rhythm topographies during motor imagery and actual movements. *Brain Topography*, 2000, vol. 12, no. 3, p. 177-186.
- [18] BAI, O., LIN, P., VORBACH, S., FLOETER, M. K., HATTORI, N., HALLETT, M. A high performance sensorimotor beta rhythm-based brain-computer interface associated with human natural motor behavior. *Journal of Neural Engineering*, 2008, vol. 5, no. 1, p. 24-35.
- [19] MICHELON, P., VETTEL, J. M., ZACKS, J. M. Lateral somatotopic organization during imagined and prepared movements. *Journal of Neurophysiology*, 2006, p. 811-822.
- [20] DOLEŽAL, J., ŠTASTNÝ, J., SOVKA, P. Recognition of direction of finger movement from EEG signal using Markov models. In *Proceedings of the 3rd European Medical & Biological Engineering Conference (EMBECE '05)*. 2005, vol. 11, no. 1, p. 1492-1492.
- [21] RAMOSER, H., MULLER-GERKING, J., PFURTSCHELLER, G. Optimal spatial filtering of single trial EEG during imagined hand movement. *IEEE Transactions on Rehabilitation Engineering*, 2000, vol. 8, no. 4, p. 441-446.
- [22] GARCIA, G. N., EBRAHIMI, T., VESIN, J. M. Support vector EEG classification in the Fourier and time-frequency correlation domains. In *First International IEEE EMBS Conference on Neural Engineering*. 2003, p. 591-594.
- [23] PFURTSCHELLER, G., SCHERER, R. The self-paced Graz brain-computer interface: methods and applications. *Computational Intelligence and Neuroscience*, 2007, 9 pages.
- [24] MAHMOUDI, B., ERFANIAN, A. Electro-encephalogram based brain-computer interface: improved performance by mental practice and concentration skills. *Medical and Biological Engineering and Computing*, 2005, vol. 44, no. 11, p. 959-969.
- [25] LIU, Y., SHARMA, M., GAONA, CH. M., BRESHEARS, J. D., ROLAND, J., FREUDENBURG, Z. V., WEINBERGER, K. Q., LEUTHARDT, E. C. Decoding ipsilateral finger movements from ECoG signals in humans. *Advances in Neural Information Processing Systems*, 2010, vol. 23, p. 1468-1476.
- [26] VUCKOVIC, A., SEPULVEDA, F. Delta band contribution in cue based single trial classification of real and imaginary wrist movements. *Medical and Biological Engineering and Computing*, 2008, vol. 46, no. 6, p. 529-539.
- [27] GU, Y., DREMSTRUP, K., FARINA, D. Single-trial discrimination of type and speed of wrist movements from EEG recordings. *Clinical Neurophysiology*, 2009, vol. 120, no. 8, p. 1596-1600.
- [28] DOLEŽAL, J., ŠTASTNÝ, J., SOVKA, P. Classification algorithms comparison for EEG movement recognition. In *19-th Biennial International EURASIP Conference Biosignal*, 2008, 5 pages.
- [29] STANČÁK, A. The electroencephalographic β synchronization following extension and flexion finger movements in humans. *Neuroscience Letters*, 2000, vol. 284, p. 41-44.
- [30] FETZ, E. Volitional control of neural activity: implications for brain-computer interfaces. *Journal of Physiology*, 2007, vol. 579, no. 3, p. 571-579.
- [31] STANČÁK, A. Event-related desynchronization of the μ rhythm in E/F finger movements. *Clinical Neurophysiology at the Beginning of the 21st Century, Supplements to Clinical Neurophysiology*, 2000, vol. 53, p. 210-214.

- [32] STANČÁK, A., PFURTSCHELLER, G. The effects of handedness and type of movement on the contralateral preponderance of μ -rhythm desynchronization. *Electroencephalography and Clinical Neurophysiology*, 1996, vol. 99, no. 2, p. 174-182, 1996.
- [33] STANČÁK, A., RIM, A., PFURTSCHELLER, G. The effects of external load on movement-related changes of the sensorimotor EEG rhythms. *Electroencephalography and Clinical Neurophysiology*, 1997, vol. 102, no. 6, p. 495-504.
- [34] KUHLMAN, W. N. Functional topography of the human μ rhythm. *Electroencephalography and Clinical Neurophysiology*, 1978, vol. 44, p. 83-93.
- [35] PFURTSCHELLER, G., STANČÁK, A., NEUPER, C. Post-movement beta synchronization. A correlate of an idling motor area? *Electroencephalography and Clinical Neurophysiology*, 1996, vol. 95, no. 4, p. 281-293.
- [36] SUBASI, B. Selection of optimal AR spectral estimation method for EEG signals using Cramer-Rao bound. *Computers in Biology and Medicine*, 2007, vol. 37, no. 2, p. 183-194.
- [37] DOLEŽAL, J., ŠŤASTNÝ, J., SOVKA, P. Modelling and recognition of movement related EEG signal. *Applied Electronics*, 2006, p. 27-30.
- [38] DOLEŽAL, J., ŠŤASTNÝ, J., SOVKA, P. Recording and recognition of movement related EEG signal. *Applied Electronics*, 2009, p. 95-98.
- [39] PETRE, P. G., EUGEN, L. On the influence of individual features coefficient over speaker recognition. *Technical University, Cluj-Napoca*, 3 pages, 2003.
- [40] MARKEL, J. D., GRAY, A. H. *Linear Prediction of Speech*. Springer Verlag, 288 pages, 1976.
- [41] YOUNG, S. J. HTK reference manual. *Cambridge University Engineering Department*, 1993.
- [42] RABINER, L. A tutorial on hidden Markov models and selected application in speech recognition. *Proceedings of the IEEE*, 1989, vol. 77, p. 257-286.
- [43] REZEK, I., ROBERTS, S. Ensemble hidden Markov models with extended observation densities for biosignal analysis. *Probabilistic Modeling in Bioinformatics and Medical Informatics*, 2005, p. 419-450.
- [44] ŠŤASTNÝ, J., SOVKA, P. High-resolution movement EEG classification. *Computational Intelligence and Neuroscience*, 2007, 12 pages.
- [45] ŠŤASTNÝ, J., SOVKA, P., STANČÁK, A. EEG signal classification: introduction to the problem. *Radioengineering*, 2003, vol. 12, no. 3, p. 51-55.
- [46] ŠŤASTNÝ, J., SOVKA, P., STANČÁK, A. EEG signal classification. In *Proceedings of the 23rd Annual International Conference of the IEEE Engineering in Medicine and Biology Society*, 2001, vol. 2, p. 2020-2023.
- [47] SITARAM, R., ZHANG, H., GUAN, C., THULASIDAS, M., HOSHI, Y., ISHIKAWA, A., SHIMIZU, K., BIRBAUMER, N. Temporal classification of multi-channel near infrared spectroscopy signals of motor imagery for developing a brain-computer interface. *NeuroImage*, 2007, vol. 34, no. 4, p. 1416-1427.
- [48] LOTTE, F., CONGEDO, M., LECUYER, A., LAMARCHE, F., ARNALDI, B. A review of classification algorithms for EEG-based brain-computer interfaces. *Journal of Neural Engineering*, 2007, vol. 4, no. 2, p. R1-R13.
- [49] JAIN, K., DUIN, W., MAO, J. Statistical pattern recognition: a review. *IEEE Transactions on Pattern Analysis and Machine Intelligence*, 2000, vol. 55, p. 4-37.
- [50] KAPER, M., MEINICKE, P., GROSSEKATHOEFER, U., LINGNER, T., RITTER, H. BCI competition 2003-data set IIb: support vector machines for the P300 speller paradigm. *IEEE Transactions on Biomedical Engineering*, 2004, vol. 51, no. 6, p. 1073-1076.
- [51] PLATT, C. Sequential minimal optimizer: A fast algorithm for training support vector machines. *Technical Report MSR-TR-98-14*, Microsoft Research, Redmond, 21 pages, 1998.
- [52] KALCHER, J., FLOTZINGER, D., PFURTSCHELLER, G. A new approach to a Brain-Computer-Interface (BCI) based on Learning Vector Quantization (LVQ3). In *Proceedings of the Annual International Conference of the IEEE*, 1992, vol. 4, p. 1658-1659.
- [53] VALFREDO, P., LOPES, S. Detection of movement-related desynchronization of the EEG using neural networks. In *Proceedings of the 22rd Annual EMBS International Conference*. 2000, vol. 2, p. 1372-1376.
- [54] HOLLMEN, J., TRESP, V., SIMULA, O. A learning vector quantization algorithm for probabilistic models. In *Proceedings of EUSIPCO 2000 X European Signal Processing Conference*, 2000, vol. 2, p. 721-724.
- [55] BOŘIL, T. Toolkit for EASYS2 EEG data format processing in Matlab, EEGLAB and sLoreta environment. In *Proceedings of the 8th Czech-Slovak Conference Trends in Biomedical Engineering*. 2009.
- [56] FRIEDMAN, J. H. On bias, variance, 0/1-loss, and the curse-of-dimensionality. *Data Mining and Knowledge Discovery*, 2004, p. 55-77.
- [57] KOHAVI, R. A study of cross-validation and bootstrap for accuracy estimation and model selection. In *Proceedings of the International Joint Conference on Artificial Intelligence*. 1995, p. 1137-1145.

About Authors

Jaromír DOLEŽAL was born in Prague, the Czech Republic in 1982. He received his M.Sc. degree in biomedical engineering from the Faculty of Electrical Engineering of the Czech Technical University (FEE CTU) in 2008. He is a Ph.D. student of the Circuit Theory Department, FEE CTU. His research interests include signal processing, information systems design, and others.

Jakub ŠŤASTNÝ was born in Prague, the Czech Republic in 1978. He received M.Sc. degree in electrical engineering from the FEE CTU, Prague in 2002; in 2001 he was awarded Hlávka's Prize and received Ph.D. degree in 2006. His current research interests include biosignal processing, signal classification techniques, blind source separation, silicon DSP architectures, and others.

Pavel SOVKA received the M.Sc. and Ph.D. degrees in electrical engineering from FEE CTU, Prague, in 1981 and 1986, respectively. From 1985 to 1991 he worked in the Institute of Radioengineering and Electronics of the Czech Academy of Science, Prague. In 1991 he joined the Department of Circuit Theory, FEE CTU. He has been Professor since 2000. Among his current research interest the application of adaptive system to noise and echo cancellation, biological signal analysis, change-point detection, and signal separation can be found.